

## Molecular Dynamics Simulation on the Interaction of R290 and POE Lubricants

XING Meibo<sup>1\*</sup>, DENG Qiao<sup>1</sup>, ZHANG Cancan<sup>2\*</sup>, ZHANG Ning<sup>1</sup>

1. Beijing Engineering Research Center of Sustainable Energy and Buildings, School of Environment and Energy Engineering, Beijing University of Civil Engineering and Architecture, Beijing 100044, China

2. MOE Key Laboratory of Enhanced Heat Transfer and Energy Conservation, Beijing Key Laboratory of Heat Transfer and Energy Conversion, Beijing University of Technology, Beijing 100124, China

© Science Press, Institute of Engineering Thermophysics, CAS and Springer-Verlag GmbH Germany, part of Springer Nature 2025

**Abstract:** In this work, the interactions between the environmentally friendly refrigerant propane (R290) and Polyol Ester (POE) including solubility parameters, diffusion coefficients, binding energies, and radial distribution functions were investigated using molecular dynamics (MD). Specifically, the effect of chain length of Pentaerythritol esters (PEC) as the representative component of POE on the interaction of PEC/R290 was discussed. The solubility parameters difference exhibits the PEC and R290 are more easily miscible as increasing chain length of PEC, and there is plateau as the chain lengths is above 8 units. In addition, it was also found that solubility parameters are various for the isomers due to the different spatial structure. Moreover, the presence of PEC would reduce the diffusion coefficient of R290 in the mixed system of R290/lubricant with the reduction of 20% on average. It is also found that van der Waals forces are dominant in the R290/PEC system. The PEC molecules start to be bound to the H atoms of R290 at the first neighbor shell layer with a radius of 0.219 nm. Finally, the molecular simulation model of POE22 considering various actual components was innovatively developed. The results showed that the solubility of R290 with typical POE lubricant is affected by the composition and proportions of based oil and additives.

**Keywords:** solubility; molecular dynamics simulation; R290; POE

### 1. Introduction

The increasing attention to environmental protection and global warming has made developing efficient and environmentally friendly refrigerants with low Ozone Depletion Potential (ODP) and low Global Warming Potential (GWP) a key issue for the sustainable development of the refrigeration and air conditioning industry. Among numerous alternative refrigerants, propane (R290) as a natural refrigerant has become a promising refrigerant due to its zero ODP, low GWP,

good thermal conductivity, high volumetric cooling capacity [1, 2], and has replaced R22 or R410A which are commonly used in air conditioning [3–5].

However, one of the challenges in the application of environmentally friendly refrigerants is the solubility of the new refrigerant with the lubricant. In the compression of refrigeration system, the refrigerant comes into compressor and directly contacts with the lubricant. The solubility of refrigerant with lubricant can affect the lubricants property of compressor and heat transfer characteristics of heat exchangers, thereby affecting the

Received: May 31, 2024  
AE: HAN Xiaohong

Corresponding author: XING Meibo;  
ZHANG Cancan

E-mail: xingmeibo@bucea.edu.cn  
zcc@bjut.edu.cn

[www.springerlink.com](http://www.springerlink.com)

Nomenclature			
$\Delta$	Solubility parameter/(J·cm <sup>-3</sup> ) <sup>0.5</sup>	PEC	Pentaerythritol esters
$D$	Diffusion coefficient/cm <sup>2</sup> ·s <sup>-1</sup>	POE	Polyol Ester
$E$	Energy/kJ·mol <sup>-1</sup>	RDF	Radial distribution function
Abbreviation		R290	Refrigerant propane
HFCs	Hydrofluorocarbons	Subscripts	
MD	Molecular dynamics	cho	Cohesive energy
MSD	Mean square displacement	inter	intermolecular
NPT	Number, Pressure, Temperature	intra	intramolecular
NVT	Number, Volume, Temperature		

performance and stability of refrigeration system. Sun et al. [6] found that the enthalpy changes of the refrigerant decrease with an increase in the mass fraction of circulating lubricants; meanwhile that the unevaporated amount of refrigerant rises with the increased mass fraction of circulating lubricants. Youbi-Idrissi et al. [7] studied R407C/POE mixtures and found that the unevaporated amount of refrigerant at the outlet side of the evaporator may be high when the refrigerant-oil solubility rises, which may lead to a reduction in evaporator performance. Yang et al. [8] reported that the thermal efficiency of a cycle using R1336mzz(E) and R1234ze(Z) was 11.4% and 3.1% lower than that of a cycle using R245fa. One of the main reasons for this result is the difference in solubility between different refrigerants and lubricants, which in turn affects the sealing performance of the compressor. There are different requirements for the solubility of the lubricant and the refrigerant at different locations in the system, at the inlet of the return line, it is required that the refrigerant and lubricant can be well mixed and returned to the compressor to ensure reliability [9]; at the outlet of the compressor, the refrigerant and lubricant are separated efficiently so that as little lubricant as possible enters the heat exchanger to improve heat transfer efficiency [10]. The working temperature and pressure of the refrigerant in each component of the refrigeration system are different. In order to consider the solubility of the refrigerant and the lubricant comprehensively, the solubility of the refrigerant and the lubricant should be analyzed for multiple working conditions. Therefore, there is need to study the interaction of hydrocarbon refrigerants such as R290 with lubricants since the appropriate solubility is essential for high performance and system reliability.

Polyol Ester (POE) lubricants synthesized from renewable resources are widely used in refrigeration systems due to their good environmental performance, thermal stability, and miscibility with refrigerants [11,12]. Neto et al. [13] investigated the solubility, density, and liquid kinetic viscosity of isobutane and POE lubricant

mixtures in the temperature range of 10°C–60°C. Martínez-Galván et al. [14] found that the use of POE was effective in reducing the amount of R290 charged and showed better system performance than the mineral oil. Tyczewski et al. [15] also found that the use of POE in R290 refrigeration systems will have better tribological properties in compressors compared with mineral oils. It is concluded POE may be the better choice for R290 refrigeration systems in the light of the results of the existed studies, and it is worthwhile to carry out further research on it.

Usually, the solubility of refrigerants with lubricants was measured by the vapor-liquid equilibrium experiment. In recent years, molecular dynamics (MD) simulations have been widely used to study the interaction between two substances [16, 17], and have also been involved in the study of the interaction between refrigerants and lubricants, which could provide valuable insights into the solubility mechanism between refrigerants and lubricants from the properties of materials. Fouad et al. [18] using molecular modeling found that the solubility of HFOs refrigerants with Pentaerythritol esters (PEC) was weakly dependent on the structure of the PEC molecule, whereas the solubility of R600a and R744 increased with the improvement of the PEC alkyl tail length in the calculated range of PEC4 to PEC9. Sugii et al. [19] studied the solubility of the R744 and the PEC6 lubricant through molecular dynamics simulations and then the solvation structure was investigated on a molecular scale. Yu et al. [20] used MD simulation to study the interactions of the polypropylene glycol dimethyl ether lubricant with R1233zd(E).

In this work, the interaction between R290 and POE lubricants including the solubility parameter, cohesion energy density, diffusion coefficient, binding energy, and the radial distribution function were studied by molecular simulation under various saturation temperatures from 238.15 K to 345.15 K, which includes the operating temperature of domestic refrigeration and air condition. Specifically, PEC as the main component of POE, the effect of monomeric units of a polymer molecule on the

interaction of PEC/R290 was discussed. Further, the solubility of R290 with typical POE lubricant was simulated by considering various actual components of the lubricant.

## 2. Methods

### 2.1 Molecular dynamics simulation

MD simulations were performed using Material Studio 9.0 software. The COMPASS force field was utilized to model all molecules, which is widely recognized for its high accuracy in representing and predicting the conformational, structural, and thermodynamic properties of molecules as well as condensed matter [21]. A 100 ps NVT MD simulation was then conducted using a Berendsen thermostat. Subsequently, 300 ps NPT simulations were performed, and the temperature and pressure are controlled by Berendsen. the coupling times for the Berendsen thermostat and the barostat were set at 0.2 ps and 4 ps, respectively. The MD simulation trajectories were saved at intervals of 1 ps. The Coulomb force interactions were calculated using Ewald summation, while the van der Waals force interactions were estimated through summation of atom-based. The cut-off radius lengths of the different systems are set according to the principle of being less than half of the box.

### 2.2 Interaction parameters of R290/lubricants

#### 2.2.1 Solubility parameter

The solubility parameter is the amount of energy per unit volume required to overcome the intermolecular forces of the condensate to vaporize, which can be obtained by calculating the square root of the cohesive energy density. These interactions need to be overcome to dissolve when the molecules are distributed in a solvent [22], and the solubility parameter is expressed as follows [23]:

$$\delta = \sqrt{e_{\text{cho}}} = \sqrt{\frac{E}{V}} = \sqrt{\frac{U_m}{V_m}} \quad (1)$$

where  $e_{\text{cho}}$  is the cohesive energy density;  $E$  is the cohesion energy;  $V$  is the molar volume of pure solvent;  $U_m$  is the molar evaporation energy of the polymer, and  $V_m$  is the molar volume of one repeating unit of the polymer. Theoretically, the closer solubility parameters of two substances mean the better solubility.

#### 2.2.2 Binding energy

The binding energy is numerically the negative of the interaction energy  $E$ , which is the strength of adsorption between molecules. The positive value of the binding energy signifies that the molecules are attractive to one another, while a negative value of the binding energy indicates mutual repulsion between the molecules. The binding energy is used to make predictions about the

solubility of the components of the system, which was calculated as follows:

$$E_{\text{binding}} = -E_{\text{solvation}} = E_{\text{POE}} + E_{\text{R290}} - E_{\text{POE-R290}} \quad (2)$$

where  $E_{\text{binding}}$  is the binding energy between lubricant and R290 and its value is equal to the negative of the interaction energy.  $E_{\text{POE-R290}}$  is the total energy of the POE/R290 mixed system;  $E_{\text{POE}}$  and  $E_{\text{R290}}$  are the energies of the POE and R290 systems, respectively.

#### 2.2.3 Diffusion coefficient

The process of formation of refrigerant/lubricant mixtures is closely related to molecular diffusion, which can usually be distinguished into two basic types of diffusion. One is natural convection, which typically occurs in the mixtures of hydrofluorocarbons (HFCs) and POE [24, 25]. The other is molecular diffusion, which usually occurs in hydrocarbon refrigerants and mineral oils [26, 27]. Natural convection mechanisms are characterized by the fact that the density of the refrigerant is greater than that of the oil, and the rate of refrigerant/lubricant mixture formation is usually greater than that of a single molecular diffusion mechanism. In this study, the density of R290 is less than that of POE, so the formation process of the mixture is mainly by the molecular diffusion. In the simulation of MD, the diffusion coefficient can be calculated from the slope of the mean square displacement (MSD) curve, which could be expressed as follows:

$$D = \frac{1}{6} \lim_{t \rightarrow \infty} \frac{d}{dt} \sum_{i=1}^N \langle |r_i(t) - r_i(0)|^2 \rangle \quad (3)$$

where  $r_i(t)$  is the displacement of molecule  $i$  at time  $t$ ;  $\langle \rangle$  is the average of all molecules in the system;  $r_i(0)$  is the displacement of molecule  $i$  at the starting moment;  $N$  is the number of molecules;  $D$  is the diffusion coefficient.

#### 2.2.4 Radial distribution functions

The radial distribution function (RDF) usually refers to the probability of the distribution of other particles in space for a given coordinate of the one particle. So that the radial distribution function can be used to study the order of the internal structure of substances. Its expression is as follows:

$$g(r) = \frac{dn}{\rho 4\pi r^2 dr} \quad (4)$$

where  $\rho$  is the density of the system;  $n$  is the number of particles in the system, and  $dn$  is the number of particles in a spherical shell of radius  $r$  and thickness  $dr$  number.

## 3. Results and Discussion

### 3.1 Model validation

Density is a fundamental property of substances. The density of the substance primarily relies on its temperature and pressure conditions from a macroscopic

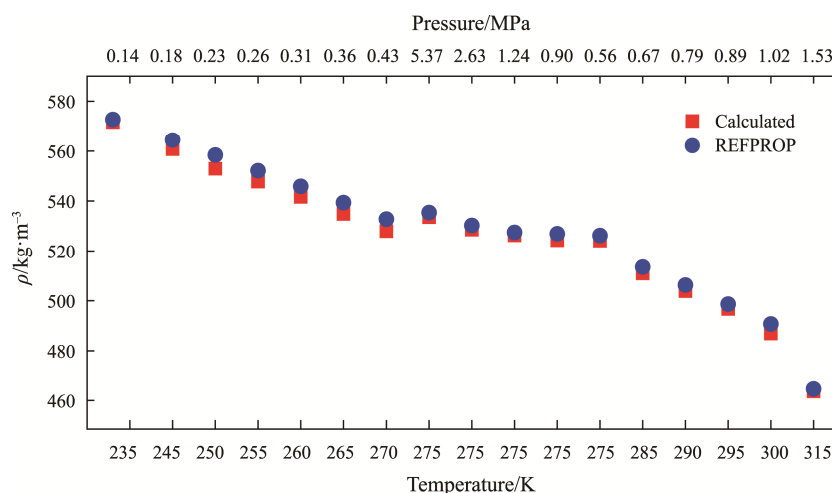


Fig. 1 Comparison of simulated and REFPROP data for liquid R290 density

point of view. On a microscopic level, the molecular structure of a substance determines its molecular weight, molecular bonding, molecular polarity, meanwhile the resulting intermolecular forces. These factors lead to variations in intermolecular distances, and consequently different densities. Therefore, precise density data served as the foundation for the accuracy of the simulation results in MD simulations.

Initially, pure R290 calculations were performed with 350 molecules; the deviation of the simulation results from the REFPROP data is small when the number of molecules is greater than 300. However, as the number of molecules increases, the time required for the simulation increases rapidly [28]. Considering the simulation accuracy and time consumption, a total of 350 molecules were used for MD simulations in this study. Construction of a cubic box was carried out using amorphous cell modules with periodic boundary conditions. The MD simulations were conducted to calculate the density of R290 within the temperature range of 235–345 K and the corresponding pressure range of 0.13–2.68 MPa. The calculated density of R290 was then compared with the density data obtained from REFPROP10.0 [29], as presented in Fig. 1. The results indicate a strong agreement between the calculated and experimental density values with relative errors consistently below 1%. This suggests that the MD simulation calculations are credible. Furthermore, an increase in the density of R290 occurs with a rise in pressure as the temperature remains constant. The density of R290 reduces at higher temperatures, which is in accordance with the thermodynamics principles.

As shown in Fig. 2, the total energy, total kinetic energy, total potential energy, and non-bonded energy of the R290 gradually converge within 300 ps under the simulated temperature conditions. The energy gradually

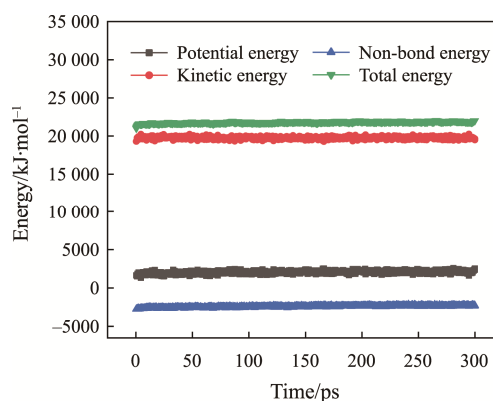


Fig. 2 Energy change of R290 during simulation

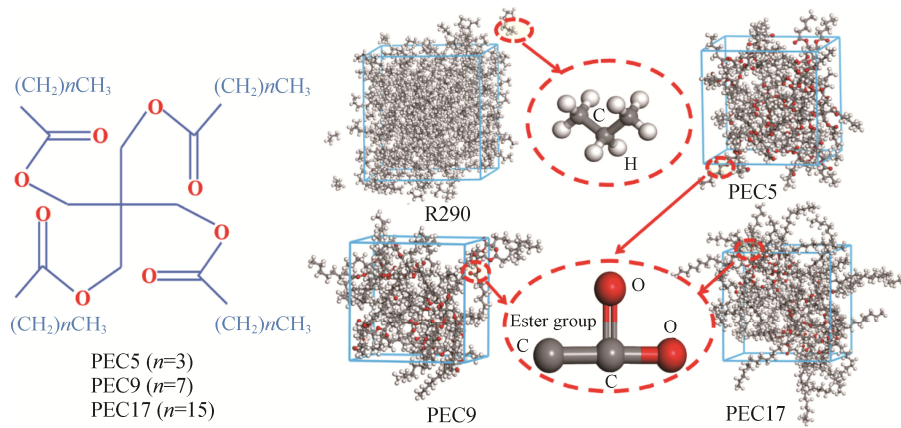
reaches a steady state within the whole system. The energy and density parameters observed in the simulation could demonstrate the applicability of the model according to the literature [30].

### 3.2 The effect of polymerization degree of PEC on the interaction

The PEC polymer molecule is the main component of POE, and many solubility studies of POE with refrigerants have focused on the PEC polymer molecule [19]. In addition, the polymerization degree and molecular weight of the polymer chains have a significant influence on the thermodynamic and solubility parameters in the polymer system [31]; the molecular structure is shown in Fig. 3. In the MD simulation, the polymerization units of PEC polymer molecules are constructed in the BUILD module. Specifically, PEC polymer molecules with polymerization degree of 4, 8 and 16 were established respectively. The geometry of each polymer molecule was firstly optimized in the Forcite module; then the

**Table 1** The different composition of simulation systems

System	Composition	Number of repeat units in a chain	Relative molecular mass of a chain	Number of chains	Number of R290
1	R290		44		350
2	PEC5	4	472	16	0
3	PEC9	8	696	14	0
4	PEC17	16	1144	10	0
5	PEC5/R290			8	350
6	PEC9/R290			5	350


**Fig. 3** Molecular structure of  $PEC_n$  and snapshots of some simulations

boxes were subjected to five cycles of annealing, which basically eliminated the local irrational structures generated during the model construction process. During the annealing process, the temperature was raised from 300 K to 500 K and then lowered to 300 K; meanwhile the temperature gradient was 50 K. Subsequent NVT calculations with MD of 100 ps were performed to pre-equilibrate the system, followed by 300 ps NPT MD simulations at different saturation temperatures with a time step of 1 fs using a Berendsen thermostat and constant pressure control. The different components of the simulated system are shown in Table 1; a snapshot of the simulations for systems 1, 2, 3 as well as 4 is shown in Fig. 3.

Fig. 4(a) shows the solubility parameter values and cohesive energy density values of R290 system at different saturation temperatures. The distribution of propane solubility parameter is between 10.2–14.2  $(J \cdot cm^{-3})^{0.5}$  at the saturation temperature range of 235 K–335 K; the calculated values of the propane solubility parameter are usually around 12  $(J \cdot cm^{-3})^{0.5}$  at normal temperatures [32], which is in line with the value of solubility parameter obtained from MD calculations. In addition, it can be seen the solubility parameter values and cohesive energy density values decrease with the increased saturation temperature. The reason for this

tendency is that the molecular thermal movement becomes stronger as the temperature rises, which leads to a rise of the intermolecular kinetic energy. At the same time, the cell volume of the system becomes larger as the temperature increases; the distance between molecules and atoms rises accordingly. Once this distance exceeds the equilibrium distance, the intermolecular force becomes an attractive force. When the intermolecular distance increases further, the intermolecular force in the system exhibits a negative work, leading to a rise in the total potential energy between the molecules. As a result, cohesion energy represents a negative value of the total intermolecular energy, so that the cohesion energy decreases with the temperature improved; the solubility parameter will decrease along with the increased cohesion energy density based on Eq. (1). In general, the solubility parameter and the cohesive energy density decrease with the improvement of saturation temperature, while the rate of decrease is different for various molecules (PEC and R290) since their volume and force field distributions are also different by different molecular weights as well as structural compositions.

Fig. 4(b) shows the calculated results of the difference in solubility parameters of R290 and PEC at various saturation temperatures versus the number of repeat units of PEC polymer molecules. It is generally known that

two substances have good solubility when the difference between their solubility parameters is less than  $4.10 (\text{J}\cdot\text{cm}^{-3})^{0.5}$  [33]. It is found the solubility parameter differences between PEC polymer molecule and R290 are all higher than  $4.10 (\text{J}\cdot\text{cm}^{-3})^{0.5}$  under each saturation temperature, indicating that PEC polymer molecule and R290 are partial miscibility. Moreover, there is a plateau for solubility parameter difference when the chain lengths of about 8 units. The average difference in solubility parameters between various polymerization degree of PEC and R290 during whole temperature range is 5.65, 5.11 and  $5.19 (\text{J}\cdot\text{cm}^{-3})^{0.5}$  for PEC5, PEC9 and PEC17, respectively, which suggests the PEC9/R290 system has the optimal solubility. The results of this study can provide guidance for the design as well as synthesis of polymers for an ideal miscibility condition. It is also found the difference of PEC5/R290 was significantly different from PEC9/R290. In order to further investigate the interaction between R290 and PEC polymer molecules, subsequent interaction analyses will focus on the interaction parameters in mixed systems 5 and 6.

In addition, the difference in solubility parameters of PEC and R290 increases with the increased saturation

temperature; Tangri et al. [34] reached similar conclusions in studying the solubility of refrigerants such as R410A, R515B and POE lubricants at saturation temperatures corresponding to the refrigeration cycle. It should be noted that the compressor is shut down after a period of operation and the temperature is low during the non-operating period; a large amount of refrigerant is soluble in the compressor lubricant and the presence of the refrigerant will have a significant impact on the anti-wear properties of the compressor lubricant [35]. Hence, the use of a heater to heat the lubricant prior to restarting the compressor can be advocated since the solubility of the refrigerant in the compressor decreases as increasing temperature.

The binding energy effectively reflects the interactions in the mixed system, and the calculated results are shown in Fig. 5. By comparing the contributions of various energy terms to the binding energy in the mixed system, it can be found that the binding energy between PEC and R290 is mainly non-bonding energy, defined as the sum of van der Waals and electrostatic energies. The electrostatic energy of the PEC polymer molecules is negative, indicating the presence of electrostatic repulsive forces in the PEC system. What's more, the

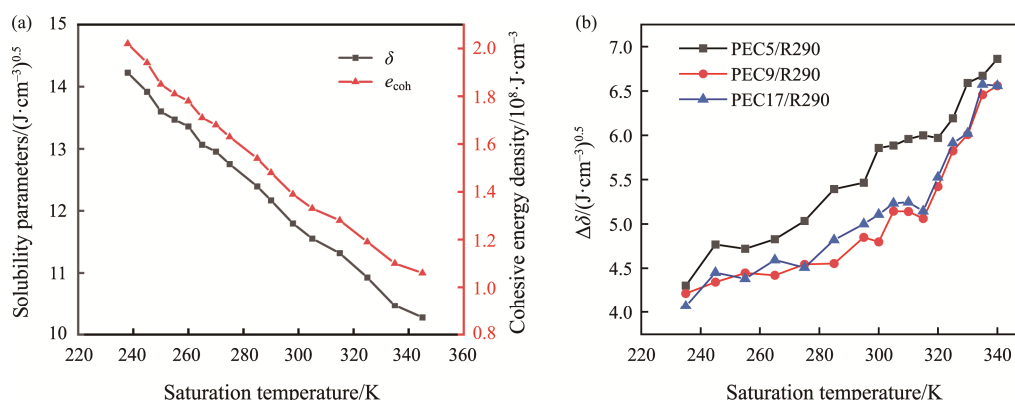


**Fig. 4** (a) Solubility parameter and cohesive energy density of R290 molecular simulation, (b) Difference of solubility parameters between R290 and PEC

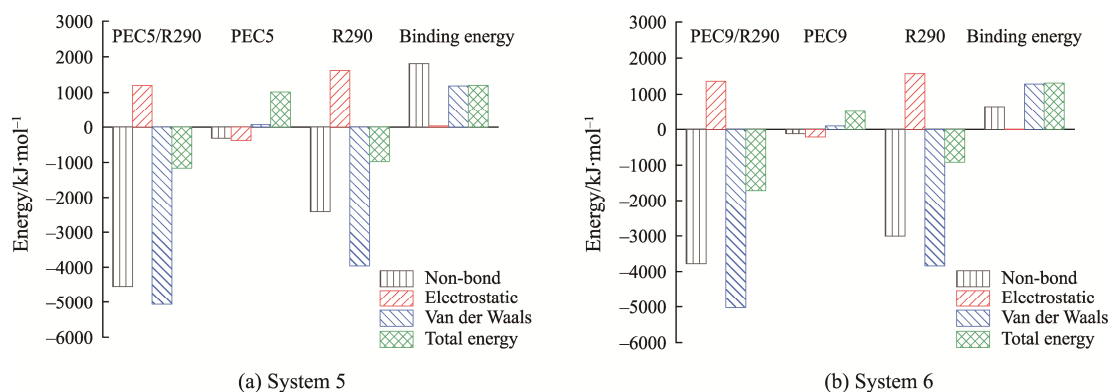


**Fig. 5** Interaction energy between PEC and R290 (275 K, 0.502 MPa)

electrostatic energy of PEC9 is lower than that of PEC5 due to the fact that the dipole moment is diluted as the degree of polymerization of the PEC polymer molecules increases. In the case of R290, the electrostatic energy is positive indicating that there is electrostatic but the value is much lower than that of the van der Waals energy. From the binding energy calculations in Fig. 5(a), it can be seen that the contribution of the van der Waals energy term ( $1283.913 \text{ kJ}\cdot\text{mol}^{-1}$ ) is larger than that of the electrostatic interaction energy term ( $1.226 \text{ kJ}\cdot\text{mol}^{-1}$ ). This indicates that the main interaction between the PEC polymer molecules and R290 is contributed by van der Waals forces. In addition, the binding energy ( $1316.651 \text{ kJ}\cdot\text{mol}^{-1}$ ) of the PEC9/R290 system was higher than that of the binding energy ( $1204.817 \text{ kJ}\cdot\text{mol}^{-1}$ ) of the PEC5/R290 system, which further confirmed the stronger interaction and better solubility between PEC9 and R290.

Fig. 6 shows the mean square displacement calculations for systems 5 and 6. The MSD of the R290 molecules in both PEC increased gradually with increasing temperature. The reason for this is that the kinetic energy of R290 is greater when the temperature is higher, which leads to an increase in the diffusion rate of

R290. The MSD of R290 molecules in PEC9 is significantly smaller in the range of simulated temperatures, indicating a greater inhibition of R290 movement in this oil. In order to obtain the R290 diffusion coefficients, a linear regression analysis was performed on each MSD curve to obtain the slope of the curve.

Fig. 6(c) shows the diffusion coefficients of the R290 component in the various systems. As can be seen from Fig. 6(c), the diffusion coefficient of R290 in the R290/PEC mixed system is smaller than that of R290 in the single R290 system, with average reductions in the order of 20%, especially at higher temperatures, where reductions reached 30%, indicating that the presence of PEC polymer molecules inhibits the diffusion of R290. It is because the addition of PEC polymer molecules enhances the interaction between the R290 components, which makes the mutual bonding closer and binds the diffusion of R290, leading to the reduction of the diffusion coefficient of R290 molecules. It is concluded that the presence of PEC polymer molecules has a certain physical constraint on the R290 components, which compresses the movement space of R290 and thus

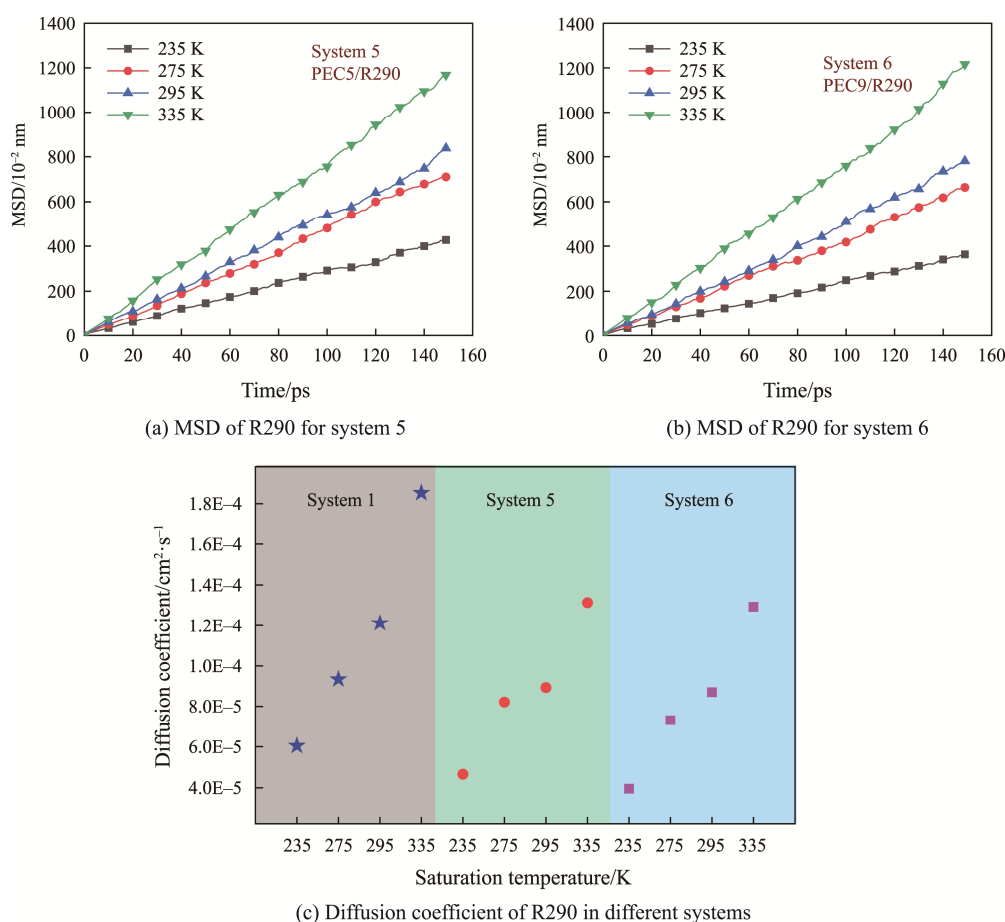


Fig. 6 MSD curves and calculated values of diffusion coefficients in different systems



reduces the diffusion coefficient of R290 molecules. In addition, PEC9 was found to have the greater effect on the diffusion rate of R290 molecules than PEC5. The reason is that the binding energy of PEC9 to R290 is greater than that of PEC5 at the same temperature, indicating that the stronger the binding of PEC9 to R290, the greater the effect of PEC9 on the diffusion rate of R290 molecules.

In order to further investigate the interaction between R290 and PEC, the radial distribution functions of PEC and PEC/R290 mixed systems were analyzed. Fig. 7 illustrates the results of the intramolecular and intermolecular radial distribution functions (RDF) for the PEC atom pairs. In Fig. 7(a), the RDF reveals several significant peaks. Firstly, the largest peak, occurring at 0.1102 nm, which corresponds to the standard length of carbon-hydrogen bond [21]. This corresponds to the carbon-hydrogen bond between C and H atoms in the PEC polymer molecule. Additionally, a second prominent peak is observed at 0.121 nm, corresponding to the carbon-oxygen double bond in the ester group. This reveals the carbon-oxygen bonds is formed within the polymer structure. Furthermore, a third notable peak appears at 0.1532 nm, indicating the presence of carbon-carbon bonds [21]. At distances of 0.217 nm,

0.245 nm, and 0.255 nm, secondary peaks are observed, representing the response of atom pairs that are not bonded in neighboring positions. Beyond 0.35 nm, the peaks diminish, as well as the intramolecular interaction curve approaches zero. This suggests that any sequential long-range structure is absent in the simulated system. Consequently, molecular structures of the constructed PEC are amorphous, which is consistent with the nature of amorphous polymers.

The RDF of PEC molecules at saturation temperature of 325 K are shown in Fig. 7(b). It is noteworthy that the positions of first and second peaks in the RDF remain the same, but the magnitude decreases rapidly compared to that of the RDF at a saturation temperature of 235 K in Fig. 7(a). This observation can be recorded due to the high compressibility of the PEC polymer molecules at lower temperatures and pressures, leading to a significant intermolecular free space when the densely packed aggregation structures are formed. However, the compressibility of the PEC polymer molecules decreases with increasing temperature as well as pressure, leading to a reduction in the free space meanwhile weaker intermolecular aggregation. On the other hand, the  $g(r)$  curves of the intermolecular atoms are shown in Fig. 7(c). In Fig. 7(c), no acute peaks were detected, which clearly

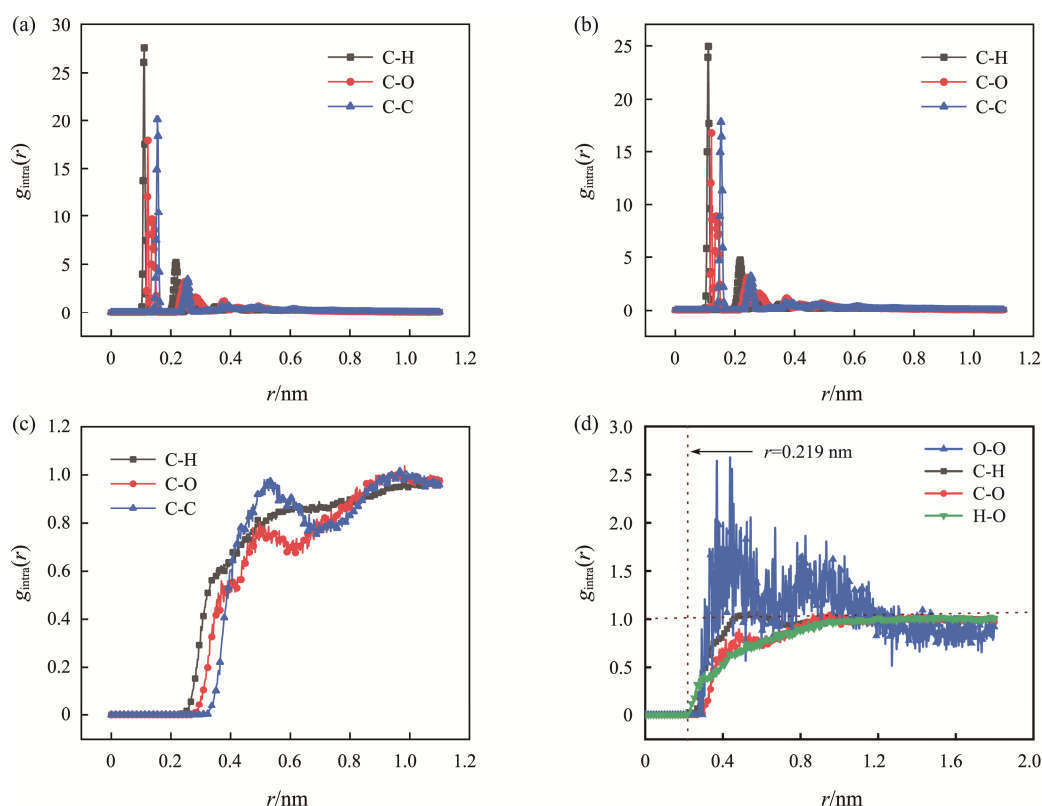


**Fig. 7** (a) RDFs of intramolecular atomic pairs of PEC polymers at 235 K, (b) RDFs of intramolecular atomic pairs of PEC polymers at 325 K, (c) RDFs of intermolecular atomic pairs of PEC polymers, (d) RDFs of intermolecular atomic pairs between PEC polymer and R290



indicates that atom pairs from different PEC molecules are not systematic over the distance  $r$ . This is also consistent with the amorphous structure of PEC polymer molecules.

To gain a greater perspective on the interactions between polymers and R290, the radial distribution function results for the intermolecular atoms between PEC5 and R290 are presented in Fig. 7(d). Among the three atom pairs, the first peak of the H-O radial distribution function in the R290-PEC5 contact contacts PEC-PEC (O-O) first, besides precedes the other atom pairs in R290-PEC5, the center C in the R290 molecule. The radius of the first neighboring shell layer, where the H-O RDF value exceeds zero, is found to be 0.219 nm. At this radius, the PEC5 molecule attaches to the H atom. For the PEC9/R290 system, this value slightly rises to 0.225 nm. This increase can be attributed to the larger number of repeating units, and it enhances the interactions between the R290 and the PEC due to the stacking factor. The findings suggest that the O atoms in the PEC chain are more easily surrounded by the H atoms in the R290 molecule than the other atoms in the PEC chain and the R290 molecule. This reveals a phase solubility between PEC and R290 under the simulated conditions, indicating that the H atoms in R290 selectively interact with the O atoms of PEC.

### 3.3 Solubility prediction of R290 with typical POE

It is well known that the POE used in refrigeration systems are usually synthetic oils mainly consisting of base oil and functionalized additives. The simulated solubility parameters will be closer to the actual values when all the constituent molecules of the POE are considered in the molecular modeling. However, MD

simulation models of POE mixtures have not been established up to now. In this work, the composition and proportions of POE22 (Viscosity of about 22 mm<sup>2</sup>/s at 40°C) were analyzed based on Gas chromatography-Mass spectrometry (GC-MS) by Jia et al. [36]. The molecular formula content in the oil is illustrated in Fig. 6. It can be found the POE22 lubricant mainly contains four kinds of ester compounds (C<sub>25</sub>H<sub>44</sub>O<sub>8</sub> 53.61%, C<sub>14</sub>H<sub>26</sub>O<sub>4</sub> 20.93%, C<sub>16</sub>H<sub>28</sub>O<sub>6</sub> 13.93%, C<sub>10</sub>H<sub>18</sub>O<sub>4</sub> 7.76%), one active diluent (C<sub>11</sub>H<sub>2</sub>O<sub>2</sub> 2.31%), and one flame retardant (C<sub>18</sub>H<sub>15</sub>O<sub>4</sub>P 0.87%). The molar fraction of these six determined components reaches 99.41%, while the molar fraction of other substances is 0.59%. Further, the MD simulation of POE22 mixtures have been conducted by the AC box with reference to the previous molecular modeling steps as shown in Fig. 8.

According to the MD simulation, the solubility parameters and cohesion energy calculations were obtained in Fig. 9. Fig. 9(a) shows the calculated solubility parameter and cohesive energy density values for POE22. It was found that the solubility parameter values and cohesive energy density values decreased with the increased saturation temperature, which is the same as the linear variation of PEC polymer molecules. It should be noticed that PEC5a (C<sub>25</sub>H<sub>44</sub>O<sub>8</sub>) possessed 53.61% in the POE22, which should be discussed as more than half of the main compositions. Meanwhile, its straight chain isomer PEC5 that has been studied as above was applied to study the effect of spatial structure on the solubility. It is found that although PEC5 and PEC5a have the same chemical molecular formula, the spatial structure is different, resulting in different charge distribution, polarity, molecular size between the two substances, and there will be differences in solubility

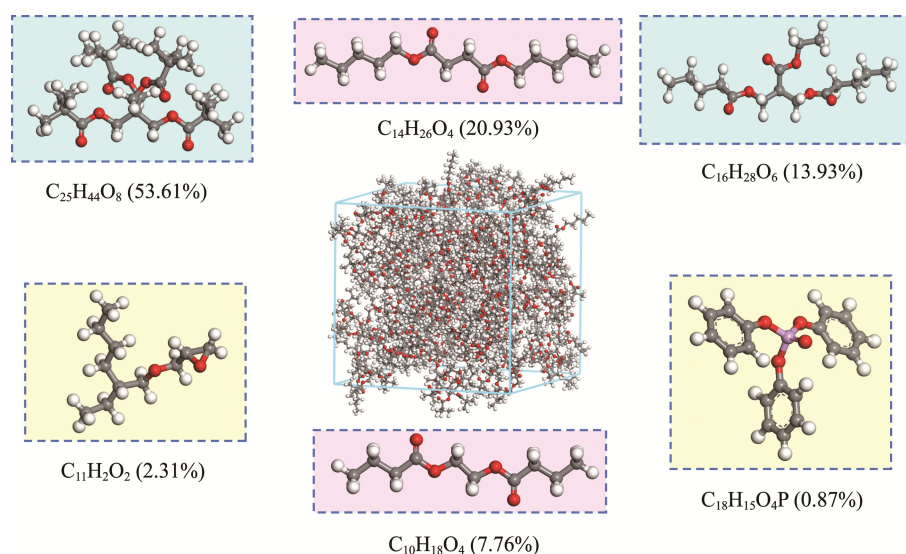
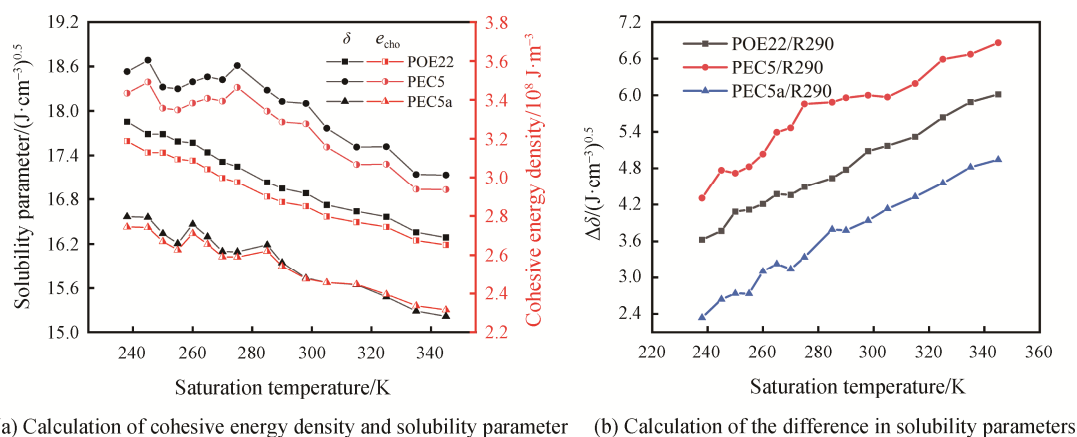


Fig. 8 Model diagrams of the six molecules and POE22 in the MD simulation



(a) Calculation of cohesive energy density and solubility parameter (b) Calculation of the difference in solubility parameters

Fig. 9 Calculated results of in MD stimulation

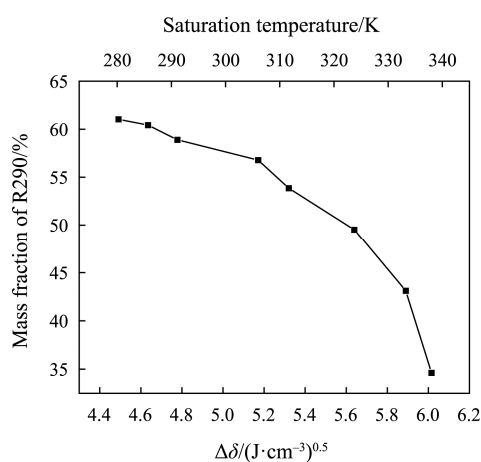


Fig. 10 Correlation between solubility and solubility parameters difference of R290/POE22

properties. The molecular structure of PEC5a is branched and the number of methyl groups in the molecule of PEC5a is higher as shown in Fig. 8, which is more similar to R290. Therefore, the solubility performance between R290 and PEC5a would be better than PEC5 based on the principle of like dissolves like [37, 38].

The differences in the solubility parameters between POE22, PEC5, PEC5a and R290 were shown in Fig. 9(b), and their average values during whole temperature range are 4.72, 5.66 and 3.60  $(\text{J}\cdot\text{cm}^{-3})^{0.5}$ , respectively. As mentioned earlier, two substances are well soluble when their solubility parameters difference is less than 4.10  $(\text{J}\cdot\text{cm}^{-3})^{0.5}$  [33]. It can be concluded that PEC5a is complete miscibility with R290; POE22 and PEC5 are partial miscibility with R290, and PEC5 has the poorer solubility with R290 than POE22. The difference in solubility parameters between POE22 and PEC5a is mainly due to the presence of several other additives in POE22.

Subsequently, the correlation between solubility and solubility parameter difference of R290/POE22 is shown

in Fig. 10. It should be noted that the solubility of R290 in the POE improved by Jia et al. [36] via the vapor-liquid equilibrium experiment. It can be seen that the mass percentage of R290 dissolved in R290/POE22 mixtures decreases as the solubility parameter difference increases. This is in agreement with the conclusion obtained in this work, which indicates the validity of the solubility rules of R290 with lubricants obtained by molecular dynamics simulation.

#### 4. Conclusions

In this work, the interaction of R290 and POE has been investigated by using molecular dynamics simulations. Firstly, the effects of polymerization degree of PEC polymer molecule as the representative component of POE on the interactions were discussed. The results indicated that the solubility parameter difference between PEC polymer molecules and R290 increases as increasing saturation temperature. Moreover, there is almost no change for the solubility parameter difference as the chain lengths is above 8 units. The presence of PEC polymers compresses the diffusion space of R290, and the decrease in diffusion coefficients of R290 is 20% on average. It is mainly van der Waals forces that govern the interaction between the PEC polymer molecules and R290. Additionally, the analysis of the radial distribution function indicates that the chemical bonding and non-bonding interactions between C-C pairs and H-C pairs in the PEC polymer molecules are consistently more pronounced at the lower saturation temperatures. The PEC molecules begin to attach to the H atoms in R290 starting from the first neighbor shell layer, which has a radius of 0.219 nm.

In MD simulation study of POE22 which is a typical polyester oil, it was found that although the main component of POE22 is PEC5a, the solubility of POE22 with R290 is lower than that of POE5a owing to the fact

that the presence of additives in the POE oils affects the solubility characteristics. Besides, it is worth noting that there are differences in solubility parameters between the PEC5 and PEC5a isomers; the molecular structure of PEC5a is more similar to that of R290, and hence PEC5a has better solubility with R290.

## Acknowledgments

This study is financially supported by Beijing Natural Science Foundation (3242015) and the Cultivation Project Funds for Beijing University of Civil Engineering and Architecture (X23041), China.

## Conflict of Interest

ZHANG Cancan is an editorial board member for Journal of Thermal Science and was not involved in the editorial review or the decision to publish this article. All authors declare that there are no competing interests.

## References

- [1] Yadav S., Liu J., Kim S.C., A comprehensive study on 21st-century refrigerants-R290 and R1234yf: A review. *International Journal of Heat and Mass Transfer*, 2022, 182: 121947.
- [2] Sánchez D., Cabello R., Llopis R., Arauzo I., Catalán-Gil J., Torrella E., Energy performance evaluation of R1234yf, R1234ze(E), R600a, R290 and R152a as low-GWP R134a alternatives. *International Journal of Refrigeration*, 2017, 74: 269–282.
- [3] Zhang Y., Liu C., Li W., Shi J., Chen J., Performance and optimization study of R290 as alternative refrigerant for R22 in low temperature heat pump system. *Journal of Physics: Conference Series*. IOP Publishing, 2021, 2108(1): 012089.
- [4] Choudhari C.S., Sapali S.N., Performance investigation of natural refrigerant R290 as a substitute to R22 in refrigeration systems. *Energy Procedia*, 2017, 109: 346–352.
- [5] Fajar T.B., Bagas P.R., Ukhi S., Alhamid M.I., Lubis A., Energy and exergy analysis of an R410A small vapor compression system retrofitted with R290. *Case Studies in Thermal Engineering*, 2020, 21: 100671.
- [6] Sun Y., Wang J., Hu Y., Effect of refrigerant/oil solubility on thermodynamic performance of the evaporator working with R600a and DME. *The Journal of Chemical Thermodynamics*, 2021, 154: 106331.
- [7] Youbi-Idrissi M., Bonjour J., Marvillet C., Meunier F., Impact of refrigerant-oil solubility on an evaporator performance working with R-407C. *International Journal of Refrigeration*, 2003, 26(3): 284–292.
- [8] Yang J., Ye Z., Yu B., Ouyang H., Chen J., Simultaneous experimental comparison of low-gwp refrigerants as drop-in replacements to R245fa for organic Rankine cycle application: r1234ze(Z), R1233zd(E), and R1336mzz(E). *Energy*, 2019, 173: 721–731.
- [9] Wu J., Duan J., Li X., et al., Experimental study on the oil return characteristics of miscible or partially miscible oil in R290 room air conditioners. *Applied Thermal Engineering*, 2021, 182: 115727.
- [10] Yao L., Wang Q., Su D., et al., Effect of lubricating oil on refrigerant distribution in microchannel heat exchangers: A Review. *International Conference on Applied Energy*, 2020, Paper ID: 433.
- [11] Ma R., Ye Y., Ma X., et al., Flow characteristics of a refrigerant-oil mixture in a vapor compression heat pump heat exchanger for space applications. *Journal of Thermal Science*, 2022, 31(2): 407–416.
- [12] Ribeiro G.B., Barbosa Jr J., Analysis of a variable speed air conditioner considering the R-290/POE ISO 22 mixture effect. *Applied Thermal Engineering*, 2016, 108: 650–659.
- [13] Neto M.A.M., Barbosa Jr J.R., Solubility, density and viscosity of a mixture of R-600a and polyol ester oil. *International Journal of Refrigeration*, 2008, 31(1): 34–44.
- [14] Martínez-Galván I., González-Maciá, J., Corberán J.M., Royo-Pastor R., Oil type influence on the optimal charge and performance of a propane chiller. *International Journal of Refrigeration*, 2011, 34(4): 1000–1007.
- [15] Tyczewski P., Zwierzycki W., Research works on the influence of substituting the refrigerant R22 with propane (R290) on the condition of the state of sliding surfaces occurring in piston compressors. *Solid State Phenomena*, 2015, 223: 163–170.
- [16] Ye M., Ye G., Liu Y., Yan Y., Guo Z., Ouyang H., Han X., Molecular dynamics investigation on the interaction of nitrile-based ionic liquids in the separation of azeotropic refrigerant R-513A. *Journal of Molecular Liquids*, 2023, 392: 123445.
- [17] Ibrahim M., Saeed T., Hekmatifar M., Sabetvand R., Chu Y., Toghraie D., Investigation of dynamical behavior of 3LPT protein-water molecules interactions in atomic structures using molecular dynamics simulation. *Journal of Molecular Liquids*, 2021, 329: 115615.
- [18] Fouad Wael A., Lourdes F.Vega., Modélisation moléculaire de la solubilité des frigorigènes à faible potentiel de réchauffement planétaire dans les lubrifiants à base d'esters de polyol. *International Journal of Refrigeration*, 2019, 103: 145–154.
- [19] Sugii T., Ishii E., Müller-Plathe F., Solubility of carbon dioxide in pentaerythritol hexanoate: molecular dynamics simulation of a refrigerant-lubricant oil system. *The Journal of Physical Chemistry B*, 2015, 119(37): 20511–20521.

- 12274–12280.
- [20] Yu B., Yang J., Shi J., Chen J., Molecular simulation on the interaction between polypropylene glycol dimethyl ether and trans-1233zd. *International Journal of Refrigeration*, 2020, 115: 48–55.
- [21] Sun H., COMPASS: an ab initio force-field optimized for condensed-phase applications overview with details on alkane and benzene compounds. *The Journal of Physical Chemistry B*, 1998, 102(38): 7338–7364.
- [22] Hildebrand J.H., Scott R.L., Solutions of nonelectrolytes. *Annual Review of Physical Chemistry*, 1950, 1(1): 75–92.
- [23] Hu D., Sun S., Yuan P., Zhao L., Liu T., Evaluation of CO<sub>2</sub>-philicity of poly (vinyl acetate) and poly (vinyl acetate-alt-maleate) copolymers through molecular modeling and dissolution behavior measurement. *The Journal of Physical Chemistry B*, 2015, 119(7): 3194–3204.
- [24] Leung M., Jotshi C.K., Goswami D.Y., Shah D.O., Gregory A., Measurements of absorption rates of HFC single and blended refrigerants in POE oils. *HVAC&R Research*, 1998, pp. 2141–2151.
- [25] Prata A.T., Barbosa J.R., The thermodynamics, heat transfer and fluid mechanics role of lubricant oil in hermetic reciprocating compressors. In: *Processing of 5th International Conference on Heat Transfer, Fluid Mechanics and Thermodynamics*, Paper: K6, 2007.
- [26] Barbosa J.R., Thoma S.M., Moise's A., Neto M., Prediction of refrigerant absorption and onset of natural convection in lubricant oil. *International Journal of Refrigeration*, 2008, 31: 1231–1240.
- [27] Fukuta M., Yanagisawa T., Omura M., Ogi Y., Mixing and separation characteristics of isobutane with refrigeration oil. *International Journal of Refrigeration*, 2005, 28: 997–1005.
- [28] Xu Z., Wang Z., Xia X., Li X., Chen Y., Yi Q., Molecular dynamics simulation of homogeneous condensation and thermophysical properties of R245fa/R141b. *Applied Thermal Engineering*, 2024, 236: 121627.
- [29] Lemmon E., Bell I., Huber M., NIST standard reference database 23: reference fluid thermodynamic and transport properties-REFPROP, Version 10.0, National Institute of Standards and Technology Standard Reference Data Program, Gaithersburg, 2018.
- [30] Gao Y., Tian W., Zhu J., Liao M., Xie Y., Study on compatibility mechanism of plasticizer and asphalt based on molecular dynamics. *Materials & Design*, 2023, 228: 111827.
- [31] Fu Y., Liao L., Yang L., Lan Y., Mei L., Liu Y., Hu S., Molecular dynamics and dissipative particle dynamics simulations for prediction of miscibility in polyethylene terephthalate/poly lactide blends. *Molecular Simulation*, 2013, 39(5): 415–422.
- [32] Prausnitz J.M., Edmister W.C., Chao K.C., Hydrocarbon vapor-liquid equilibria and solubility parameter. *AIChE Journal*, 1960, 6(2): 214–219.
- [33] Li C., Fan S., Xu T., Method for evaluating compatibility between SBS modifier and asphalt matrix using molecular dynamics models. *Journal of Materials in Civil Engineering*, 2021, 33: 04021207.
- [34] Tangri H., Purohit N., Sethi A., Hulse R., Solubility, miscibility and compatibility studies of low GWP non-flammable refrigerants and lubricants for refrigeration and air conditioning applications. *International Journal of Refrigeration*, 2023, 148: 45–63.
- [35] Górny K., Stachowiak A., Tyczewski P., Zwierzycki W., Lubricity evaluation of oil-refrigerant mixtures with R134a and R290. *International Journal of Refrigeration*, 2016, 69: 261–271.
- [36] Jia X., Wang J., Sun Y., Wang X., Hu Y., Shi Z., Guo X., Experimental study on vapor-liquid equilibrium of propane and POE lubricant oil. *Journal of Xi'an Jiaotong University*, 2020, 54(02): 78–85 (in Chinese).
- [37] Du-Cuny L., Huwyler J., Wiese M., et al., Computational aqueous solubility prediction for drug-like compounds in congeneric series. *European Journal of Medicinal Chemistry*, 2008, 43(3): 501–512.
- [38] Kuentz M., Imanidis G., In silico prediction of the solubility advantage for amorphous drugs—Are there property-based rules for drug discovery and early pharmaceutical development. *European Journal of Pharmaceutical Sciences*, 2013, 48(3): 554–562.